Inhibition of $A\beta_{1-42}$ fibrillation by chaperonins: human Hsp60 is a stronger inhibitor than its bacterial homologue GroEL

Silvia Vilasi[1]*, Rita Carrotta[1]*, Caterina Ricci[2], Giacoma Cinzia Rappa[1], Fabio Librizzi[1], Vincenzo Martorana[1], Maria Grazia Ortore[2], Maria Rosalia Mangione[1].

*These authors contributed equally to this work

1 Institute of Biophysics, National Research Council, Palermo, Italy;

2 Department of Life and Environmental Sciences, Marche Polytechnic University, Ancona, Italy.

Abstract

Alzheimer's disease is a chronic neurodegenerative disease characterized by the accumulation of pathological aggregates of amyloid beta peptide. Many efforts have been focused on understanding peptide aggregation pathways and on identification of molecules able to inhibit aggregation in order to find an effective therapy. As a result, interest in neuroprotective proteins, such as molecular chaperones has increased as their normal function is to assist in protein folding, or to facilitate the disaggregation and/or clearance of abnormal aggregate proteins. Using biophysical techniques, we evaluated the effects of two chaperones, human Hsp60 and bacterial GroEL, on the fibrillogenesis of $A\beta_{142}$. Both chaperonins interfere with $A\beta_{142}$ aggregation, but the effect of Hsp60 is more significant and correlates with its more pronounced flexibility and stronger interaction with ANS, an indicator of hydrophobic regions. Dose-dependent ThT fluorescence kinetics and SAXS experiments reveal that Hsp60 does not change the nature of the molecular processes stochastically leading to the formation of seeds, but strongly delays them by recognition of hydrophobic sites of some peptide species crucial for triggering amyloid formation. Hsp60 reduces the initial chaotic heterogeneity of $A\beta_{142}$ sample at high concentration regimes. The understanding of chaperone action in counteracting pathological aggregation could be a starting point for potential new therapeutic strategies against neurodegenerative diseases.

Keywords: Amyloid aggregation, inhibition mechanisms, Alzheimer's disease treatment, molecular chaperones, chaperonin, structural evolution, hydrophobic regions, ANS dye.

1. Introduction

Neurodegenerative diseases, including Alzheimer's disease, Parkinson's disease, Hungtington's disease, amyotrophic lateral sclerosis, and prion disease, are characterized by the accumulation of protein aggregates into inclusion bodies and/or plaques. The protein deposition represents the final step of protein misfolding and aggregation intricate pathways that eludes complex cellular control systems designed to maintain proteostasis. In particular, Alzheimer's disease (AD) represents the most common form of dementia in the elderly. The incidence of AD is growing every day, stressing the need for an effective treatment. AD is characterized by the aggregation and accumulation of amyloid beta (Aβ) peptide in well-ordered, β-sheet rich fibers in the extracellular compartment. Although Aβ fibers are the hallmark of AD, much evidence indicates that small oligomers (spherical oligomers and protofibrils) are the causative primary toxic species[1-3]. These oligomers are heterogeneous and intrinsically unstable; they can differ in size, formation pathways, mechanisms of toxicity[4-6], and are believed to be able to move among the different cellular compartments and the extracellular space[7, 8]. The oligomer structural variability and the complexity of the aggregation pathways, as well as the different toxicity mechanisms of diverse aggregates, may help to explain why therapeutic strategies against AD are not actually effective, despite huge efforts that have been made in the last decades. Recently, control systems to stop the protein aggregation and thus maintain proteostasis have received a great attention as potential neuroprotective systems. Because protein aggregation is a common cellular event, cells counteract aggregation by a number of known mechanisms (molecular chaperones, ubiquitin-proteasome system, endoplasmic reticulum associated degradation). These mechanisms may be impaired by aging, justifying the agerelated onset of some diseases.

Chaperones are a class of ubiquitous proteins highly conserved throughout evolution. They are crucial in many physiological cellular processes, such as correct protein assembly or folding, targeting and transport[9-12]. Thus, due to their role in folding, they can play a pivotal role in fighting pathological events involved in many neurological disorders[13-16]. In fact, the incorrectly folded proteins origin protein supramolecular assembly strictly related to neurodegenerative diseases[17-19]. Moreover, chaperones can prevent the pathological consequences of aggregation by interacting with unfolded or aggregated proteins involved in pathological conditions, immobilizing (holding chaperones), or dissolving (disaggregating chaperones)[20] them. Among chaperones, a very interesting class is represented by chaperonins: complex protein machines organized into a single or double oligomeric structure of 7-9 monomers that mainly assist correct protein folding and assembly[21, 22]. Chaperonins are classified in Group I or II. The Group I chaperonins are assisted by co-chaperonins[12], smaller proteins organized in ordered structures that properly guide chaperonin activity. The folding activity

of chaperonins is usually triggered by ATP but a second passive mechanism can also occur. In the absence of ATP, chaperonins can sequester misfolded or aggregated proteins, by an "amateur mechanism"[23-25]. This multifunctional ability, due to the presence of highly flexible regions constituting the active sites for substrate binding, clearly requires further investigation, eventual with the goal of using chaperones and chaperonins as protective agents and avoiding the consequences of pathological aggregation associated with neurodegenerative disorders[18, 23, 26-28]. Certainly, a better understanding of chaperone action on protein aggregation may illuminate structure-toxicity mechanisms and lead to the implementation of effective treatments for AD.

In this work, we evaluate the effect of the Group I human chaperonin Hsp60 and its bacterial homolog GroEL on the $A\beta_{142}$ peptide fibrillation. In previous studies, some of us showed that human chaperonin Hsp60 was able to inhibit $A\beta_{140}$ amyloid fibril formation in the absence of ATP and co-chaperones, by an amateur mechanism[24]. In fact, evidence supports the idea that Hsp60 is able to sequester *in pathway* amyloid seeds, crucial for the subsequent amyloid assembly, thus inhibiting fibrils formation. In a recent study, some of us also reported that the presence of Hsp60 prevents a model membrane from the stiffening caused by the interaction with amyloid β-peptide species, through a wipe out action against the reactive species [24, 25]. Notably, many studies show evidence of variability in the fibrillation pathways that control pathological aggregation of $A\beta_{1-40}$ and $A\beta_{1-42}$ peptides[29-32]. The different behaviors start from different arrangements of the initial nucleus, and are emphasized during the evolution of kinetics. This is characterized by a faster aggregation and a strong secondary nucleation in the case of $A\beta_{1-42}$, and is reflected in a different structural organization of the final fibrils. Probably these differences correlate with the higher frequency of $A\beta_{1-42}$ found in AD patients' plaques with respect to $A\beta_{1-40}$. The inhibition strategies of $A\beta_{1-42}$ toxic species formation are considered a valid disease-modifying therapy for AD and analytical approaches have been developed for identifying modulators of the specific $A\beta_{1-42}$ aggregation steps [29, 33-35]. According to that, the evaluation of Hsp60 action on $A\beta_{1-42}$ peptide inhibition is an interesting issue to address. The suppressing action of GroEL on $A\beta_{140}$ amyloid formation has been reported in literature[36] as well as the reduction of neurotoxic effects of $A\beta_{142}$ on human stem cell-derived neuronal cultures, that has been correlated with the sequestering action of GroEL[37], highlighting the potential neuroprotective role of human chaperonin Hsp60 against AD. The two chaperonins, GroEL and Hsp60, differ in their oligomer organization and stability[38-40]. In fact, GroEL is only found in a tetradecameric conformation, while Hsp60 exhibits a dynamic heptamer/tetradecamer equilibrium[38, 39, 41, 42]. Moreover, our previous studies confirmed the hypothesis that the evolution from bacterial GroEL to human Hsp60 generated a higher flexibility and a smaller stability to the human protein, both in the

precursor form, bearing the N-terminal Mitochondrial Import Sequence (MIS) absent in bacterial GroEL[43], and in the mitochondrial form missing of MIS [38, 39].

. Here, we evaluate and compare the inhibition efficiency of Hsp60 and GroEL on the aggregation of $A\beta_{142}$, whose amyloid proliferation is dominated by secondary nucleation events[29] and has been successfully used to obtain biophysical insights on chaperones-amyloid species interactions[33, 35]. It is worth noting that, although Hsp60 and $A\beta_{1-42}$ have different physiological localizations, in pathological situations they can co-localize and directly interact. In fact, it has already been shown that Aβ accumulates in the mitochondria of AD patients [44] and it has been suggested that intracellular and mitochondrial accumulation of Aβ precedes extracellular Aβ deposition [45]. In addition, Hsp60 and Aβ peptide can directly interact in the extracellular space, because it has been shown that in pathological situations, the human chaperonin accumulates in the cytosol with mitochondrial export release [46, 47], and from the cytosol Hsp60 may reach other cellular compartments, as well as the extracellular space [48, 49]. In this work Thioflavin T (ThT) spectrofluorimetric measurements, Circular Dichroism (CD) spectroscopy, and Atomic Force Microscopy (AFM) were used to investigate the effects of both GroEL and Hsp60 chaperonins on $A\beta_{142}$ fibrillogenesis. We show that both chaperonins interfere with $A\beta_{142}$ fibrillation, the human chaperonin being more efficient. The effectiveness of a sub-stoichiometric chaperonin concentrations, the absence of ATP and co-chaperonins, as well as the dose-dependence of the inhibition effect, suggest that the two chaperonins are able to recognize and sequester the $A\beta_{1-42}$ seeds also, with an amateur mechanism similar to that previously observed for Hsp60 with $A\beta_{1-40}$ seeds[24, 25]. The different efficiency of the two chaperonins in inhibiting amyloid peptide aggregation can be ascribed to specific differences in physico-chemical-structural properties, resulting in a different surface hydrophobicity, as assessed by ANS assay, presented by the two chaperonins as determined by their different physiological oligomeric equilibrium. We further focused on the action of Hsp60, by exploring a wider range of concentrations and investigating the effect on the chaperonin in terms of structural features by Small Angle X-ray scattering (SAXS). We observed that, at high concentrations, Hsp60 is able to reduce the sample chaotic initial heterogeneity and the fibrillation process.

2. Results and discussion

Aβ$_{1–42}$ peptide aggregation kinetics in presence of chaperonins

Aβ fibrillogenesis is a very complex process, characterized by a pronounced conformational polymorphism, strongly dependent on the initial state of the sample and on the environmental conditions (pH, temperature, salts concentration)[6, 50, 51]. Moreover, the fibrillation process can vary considerably depending on the manufacturing process (recombinant or synthetic) or purification procedure[32, 52]. Regrettably, this difficult control of the peptide stocks often leads to poor reproducibility of *in vitro* data, most likely due to the presence of even extremely small amounts of pre-existing aggregates or seeds[53]. Therefore, these species must be removed or dissociated in order to obtain an "aggregate free" peptide solution. We investigated the effects of different sample preparation protocols as reported in SM, and we chose the protocol that allowed the best removal of these small seeds present in the initial sample, and hence the best reproducibility of its aggregation pattern (see SM1).

Once the protocol was established, the kinetics of Aβ$_{142}$ fibril formation was monitored in the presence and in the absence of Hsp60 and GroEL by measuring the increase of ThT fluorescence as a function of incubation time. Experiments were performed by varying the molar ratio [Chaperonin]/[Aβ$_{142}$] from 0 to 0.05 to maintain sub stoicometric levels (Figure 1). Aβ$_{1-42}$ aggregation follows the typical kinetic pattern with a lag-phase of about 20 hours, and reaches a plateau after about 30 hours.

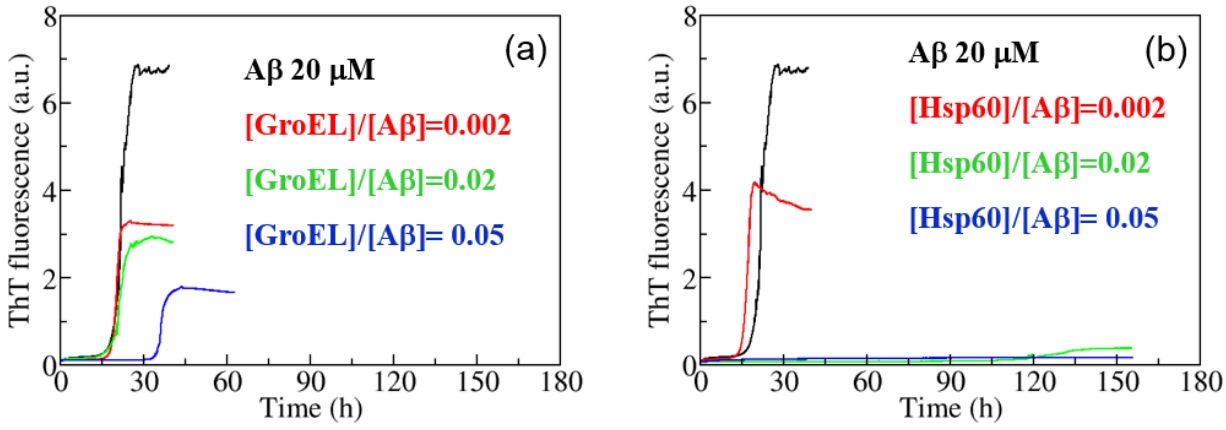

Figure 1: Dose-dependence study of GroEL (a) and Hsp60 (b) on 20 μM Aβ$_{1–42}$ amyloid aggregation, monitored by ThT fluorescence

Figure 1 shows clearly that both chaperonins are able, at relatively low doses, to interfere with the $A\beta_{1-42}$ aggregation process. However, a markedly different effect of the two chaperonins can be easily seen. The bacterial GroEL is able to reduce the final plateau value of ThT kinetics, which is related to the total final amount of fibrils and to their ThT affinity, but has a moderate effect on the lag-phase duration and on the rate of the aggregation. In fact, in the case of GroEL a significant delay of the kinetics can be observed only at the highest tested molar ratio (0.05, see the blue line in Figure 1a). In contrast, Hsp60 clearly shows a greater inhibitory effect on the fibrillation process, and at lower concentrations than GroEL. In fact, even in the sample containing Hsp60 at 0.02 molar ratio, only a very small ThT increase can be observed after an extremely long time (120 hours, see the green line in Figure 1b). Moreover, similarly to what was previously observed for $A\beta_{1-40}$[24], no ThT increase at all was observed for the whole duration of the experiment (~160 hours) in the sample with Hsp60 at 0.05 molar ratio. AFM images support the ThT results (Figure 2). Fibrillary structures were present for all samples that show an increase of ThT signal, due to β-sheet intercalation of the dye molecules.

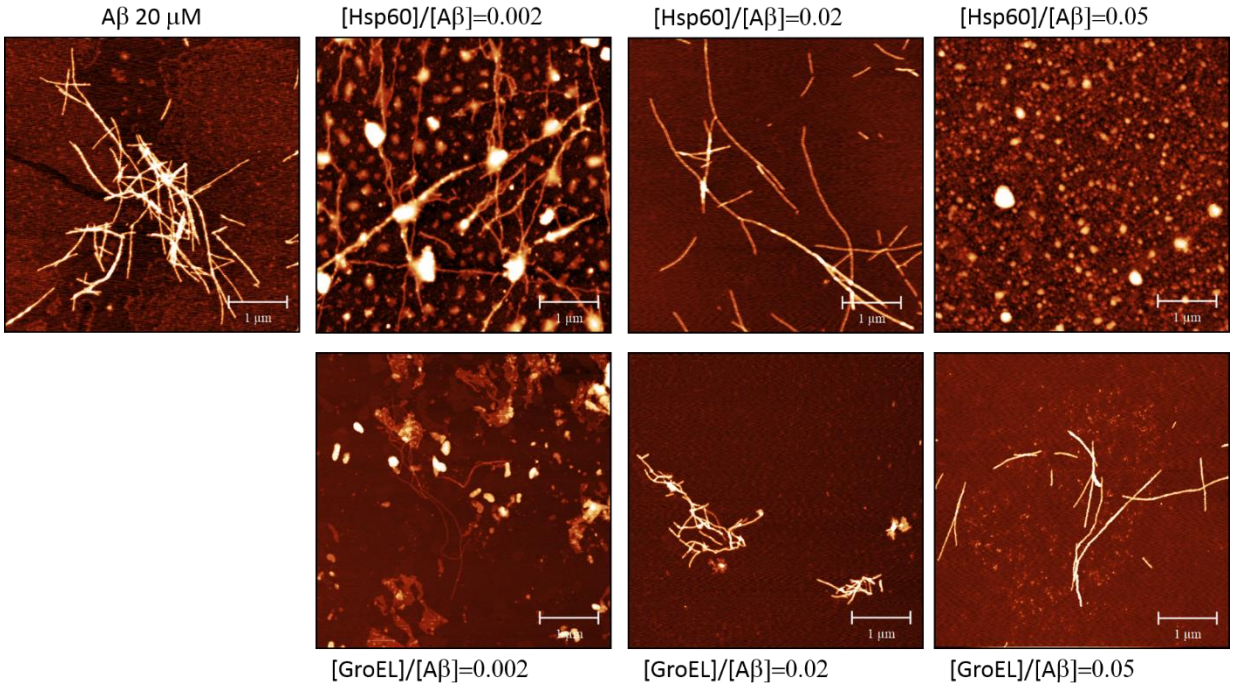

Figure 2: AFM images of $A\beta_{1-42}$ solutions at the end of the kinetics in the absence and in the presence of GroEL and Hsp60. (Scale bar 1μM).

However, for the sample [Hsp60]/[$A\beta_{1-42}$] = 0.05 which did not show any ThT signal growth, only amorphous aggregates were detected.

GroEL and Hsp60 are generally considered professional chaperones that exert their main folding action in the presence of co-chaperonins, (GroES and Hsp10 respectively) and require ATP for releasing the guest protein. However, the inhibitory effect obtained here in a sub-stoichiometric conditions, and in a concentration dependent manner without ATP and co-chaperonins, suggests a

holding, amateur mechanism specifically directed toward seeds that act to trigger the amyloid cascade[54-56]. An "amateur" mechanism has been proposed for some professional heat shock chaperones that are able to interfere with protein pathological aggregation without ATP[23, 24, 37, 57]. In previous studies, some of us showed that even without ATP and co-chaperonins, Hsp60 is able to specifically target the $A\beta_{1-40}$ species responsible for induction of amyloid protein assembly, thus acting as an amateur chaperone at sub-stoichiometric concentrations[24, 25]. Moreover, it was shown that the apical domain of GroEL is able to inhibit the amyloid fibrillation by recognizing and binding non-native protein molecules through hydrophobic interactions, however sub-stechiometric chaperonin concentrations were not used to arrest the fibrillation[58]. More recent evidence shows the protective role of GroEL, also at high concentrations, against $A\beta_{142}$ induced neurotoxicity and emphasizes the potential role of human Hsp60 in modifying the progression of AD[37].

Spectrofluorimetric assessment of chaperonins surface hydrophobicity by ANS assay

In order to explain the higher effectiveness of Hsp60 in comparison to GroEL, and to shed light on the general anti-amyloidogenic mechanisms of Hsp60, we investigated the differences in hydrophobicity between the two chaperonins using an ANS titration assay. ANS is a commonly used probe to identify hydrophobic sites and regions in proteins. In fact, ANS binding to protein hydrophobic patches is associated with an enhanced fluorescence coupled with a blue shift of the emission peak. Thus, the change in ANS emission fluorescence can be related to protein conformational changes and solvent-accessible surfaces[59, 60].

ANS was incubated with 1 µM GroEL and Hsp60 in a concentration range between 0 and 95 µM.

In Figure 3, the emission spectra for 8 µM ANS in the presence or absence of chaperonins are shown.

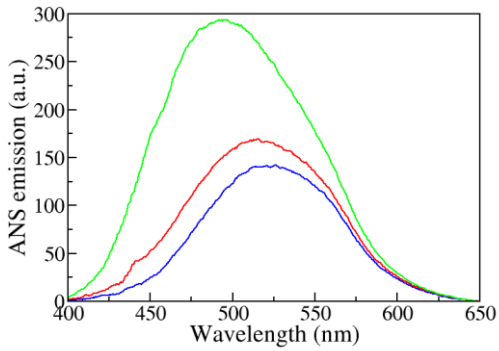

Figure 3: Fluorescence emission spectra of 8 µM ANS in the absence (blue) and in the presence of 1 M Hsp60 (green) or 1 M GroEL (red)

Notably, the presence of Hsp60 causes a significant increase of the fluorescence emission intensity with a concomitant blue shift of the peak and an obvious change in the ANS emission spectrum. In contranst, only a small blue shift and a small increase of fluorescence emission is observed in the

presence of GroEL. The different behaviors of the two chaperonins can be appreciated by evaluating the emission spectrum area, normalized for ANS concentration and suitably corrected for absorption, and the average emission wavelength λ_{av} (first moment of the spectrum) as a function of ANS concentration, as reported in Figures 4a and 4b respectively. The fluorescence signal can be considered as a linear combination of two different spectral contributions, due to the population of ANS molecules bound (*bound fraction*) to the protein and the population of free ANS (*free fraction*). At low ANS concentration, the *bound fraction* is higher than at high ANS concentration, and this brings about an increase in the overall emission spectrum area and a blue shift in λ_{av} of the probe. As evident in Figure 4 (a, b), both of these effects are much more pronounced in the case of Hsp60 with respect to GroEL. A complete analysis in terms of bound and free ANS fractions in the presence of the two chaperonins is not possible, because of the unknown emission profile and quantum yield of ANS bound to the two proteins, whose determination would require an impracticable measure of ANS fluorescence at quite high chaperonins concentrations. Nevertheless, the results reported in Figures 3 and 4 (a,b) clearly indicate a huge difference in the ANS affinity with the two proteins, suggesting the presence of a greater extension of hydrophobic regions and patches in the Hsp60 molecule. Logically, the presence of these regions could play a role in the higher Hsp60 effectiveness against $A\beta_{1\text{-}42}$ aggregation, favoring a stronger interaction with the most reactive $A\beta_{142}$ species thus increasing the ability to inhibit the peptide fibrillation more strongly.

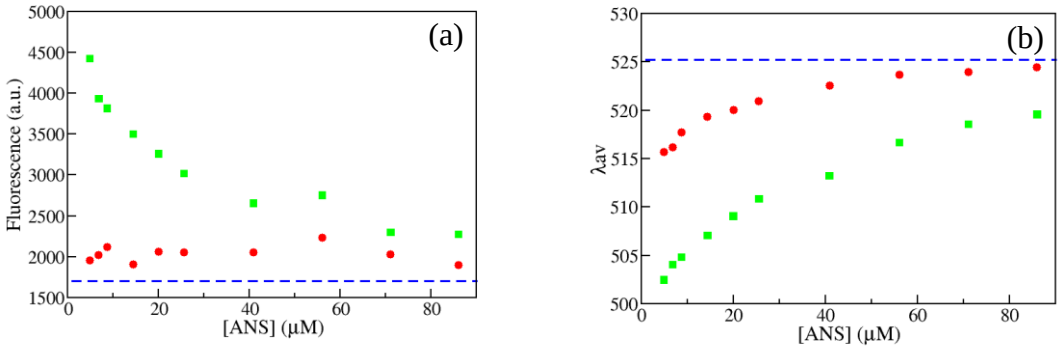

Figure 4: Fluorescence emission spectrum area normalized for the ANS concentration for the ANS free in solution (blue line) or in the presence of GroEL (red) and Hsp60 (green) as a function of ANS concentration (a). Shift of λ_{max} for ANS in the presence of GroEL (red) and Hsp60 (green) as a function of ANS concentration in comparison with λ_{max} for the ANS free in solution (blue dotted line)(b) .

This different propensity to interact with ANS can be explained considering the different structural properties of the two chaperonins. Although GroEL and Hsp60 have a very high structural homology, they exhibit some differences in structure and stability. Differently from GroEL that exists only as tetradecamer, Hsp60 is also active as a single heptameric ring[61-63]. This difference in oligomeric

structure, as part of the evolutionary pattern from bacterial to eukaryotic cells, is thought to confer a higher flexibility to the Hsp60 chaperonin complex, and an associated reduction of stability[38, 64]. These structural differences can also influence the exposed hydrophobic surfaces that trigger the recognition and selection of a substrate by the chaperonins[65, 66]. During their folding action, chaperones recognize and bind, by specific structural features, to the hydrophobic residues exposed during early stages of non-native abnormal assembly[9, 66, 67]. In fact, proteins usually bury hydrophobic regions in internally, but these regions become exposed during unfolding as well as during amyloid fibrillation. We hypothesize that both chaperonins sequester the seeds that trigger the amyloid fibrillation pathway. The higher ANS affinity for Hsp60 explains its capacity to sequester more seeds, and the increase in the ability to inhibit the $A\beta_{142}$ fibrillation.

Investigation on Hsp60 inhibition mechanism

Due to the higher effectiveness of Hsp60 in inhibiting $A\beta_{1\text{-}42}$ amyloid aggregation, we focused our attention on the mechanism of action of this chaperonin. We analyzed the effect of Hsp60 on $A\beta_{142}$ fibrillation kinetics by varying peptide concentration and maintaining the molar ratio [chaperonin]/[Aβ] at 0.016. Results are shown in Figure 5. This approach, developed for studying several protein-molecular chaperone systems, has revealed important details on the identification of the protein components targeted by the chaperones and on the aggregation steps affected[33-35]. It is evident that as the $A\beta_{1\text{-}42}$ concentration is decreased, the lag phase increases and the ThT plateau decreases (Figure 5). The inset on Figure 5 shows the half times, $T_{1/2}$, as a function of the initial concentration of $A\beta_{1\text{-}42}$ in the absence and in the presence of Hsp60. The delay of the fibrillogenesis due to the presence of Hsp60 leads to a shift of the experimental points toward higher $T_{1/2}$ values, suggesting that the chaperonin affects the availability of the seeds and therefore the onset of the secondary exponential nucleation. Moreover, the values for the scaling exponent, $\gamma = -0.65 \pm 0.06$ and $\gamma = -0.78 \pm 0.18$ for $A\beta_{142}$ alone and $A\beta_{142}$ with Hsp60, respectively, overlap within the error bar. This suggests that the inhibitory action of Hsp60 is the same at all the conditions studied, $A\beta_{1\text{-}42}$ concentration ultimately governs the onset of the kinetics and the presence of Hsp60 does not change the nature of the stochastic process leading to the formation of the seeds, but strongly delays its appearance and effect.

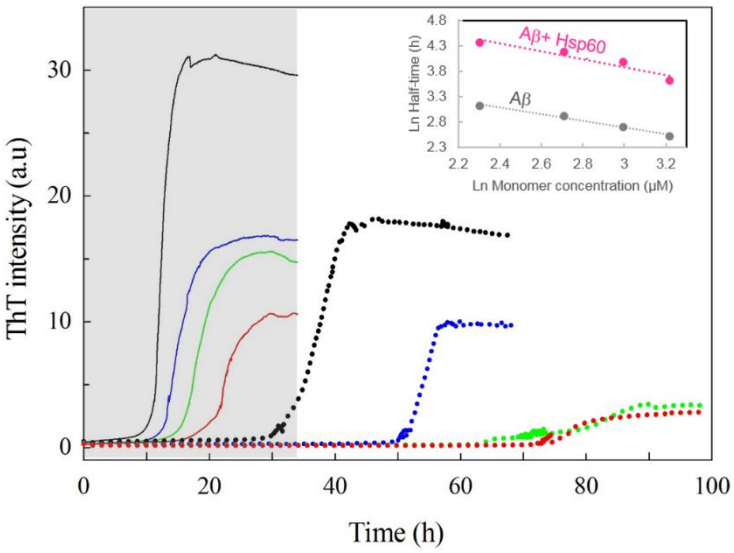

Figure 5: Amyloid aggregation kinetics monitored by ThT fluorescence for $A\beta_{1-42}$ solutions in the concentration range 25-10 μm (black 25 μM, blue 20 μM, green 15 μM, red 10 μM) in the absence (solid line and gray region) and in the presence (dotted line) of Hsp60 in a fixed chaperonin:peptide ratio of 0.016. Inset: half-times as a function of the initial $A\beta_{1-42}$ concentration in the absence (grey) and in presence of Hsp60 (pink). The exponents do not change significantly being γ=-0.65±0.06 and γ=-0.78±0.18 for Aβ and for Aβ+Hsp60, respectively

SAXS and ThT experiments at high concentrations

Finally, to further characterize the Hsp60 effect on $A\beta_{142}$ peptide fibrillation kinetics, in terms of structural features, we performed SAXS measurements. Due to the high concentration of $A\beta_{1-42}$ required for these experiments (200μM) with respect to the concentrations analyzed so far, we performed control ThT experiments at this concentration, in the presence or absence of 8 μM Hsp60 (Figure 6).

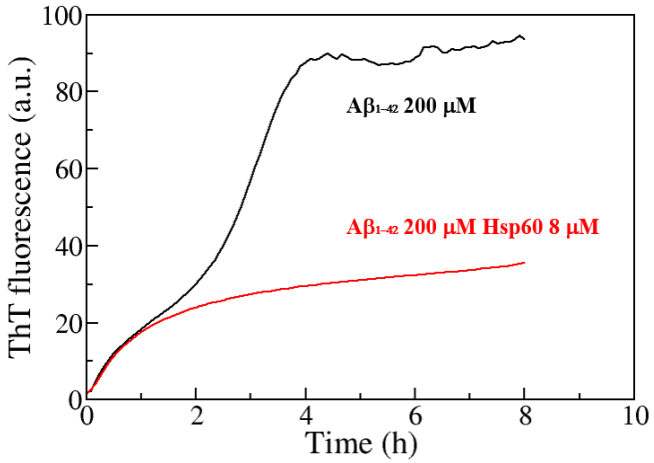

Figure 6: Amyloid aggregation kinetics monitored by ThT fluorescence for 200μM $A\beta_{1-42}$ (black), and $A\beta_{1-42}$ at the same concentration incubated with 8μM Hsp60 (red)

In the absence of chaperonin, the ThT profile appears biphasic, without any detectable lag-phase. This behavior could conceal a coexistence of events, a complicated multi-step nucleation processes, or it could result from an uncontrolled initial situation, due to the high protein concentration in solution. Although in presence of Hsp60 the ThT signal increases at the start of the kinetics, the inhibitory effect of Hsp60 on $A\beta_{1-42}$ aggregation is clear even under these conditions. The reduced growth of the ThT signal suggests a decreased extension of fibrillogenesis. SAXS experiments are in agreement with ThT results. The time evolution of the scattering intensity $I(Q)$ of 200μM $A\beta_{142}$ peptide incubated at 37 °C in the absence and in the presence of Hsp60 is shown in Figure 7. SAXS signal corresponding to the peptide alone starts from a distribution of disordered species, as evidenced by the lack of a bell-shape in the Kratky plot reported in Figure 8[68]. Due to the high peptide concentration, the starting point of the kinetic process cannot be considered to be populated just by monomers. Instead, mixture of monomers and oligomers is present in solution, that rapidly evolves over time, as seen by the increase in the intensity at $Q \approx 0$, indicating aggregate growth. In contrast, the $A\beta_{1-42}$ sample with Hsp60, even though it starts as a heterogeneous mixture, is partly inhibited in its evolution, since the differences between the features of the starting and the end curves are less pronounced with respect to $A\beta_{142}$ alone (Figure 7).

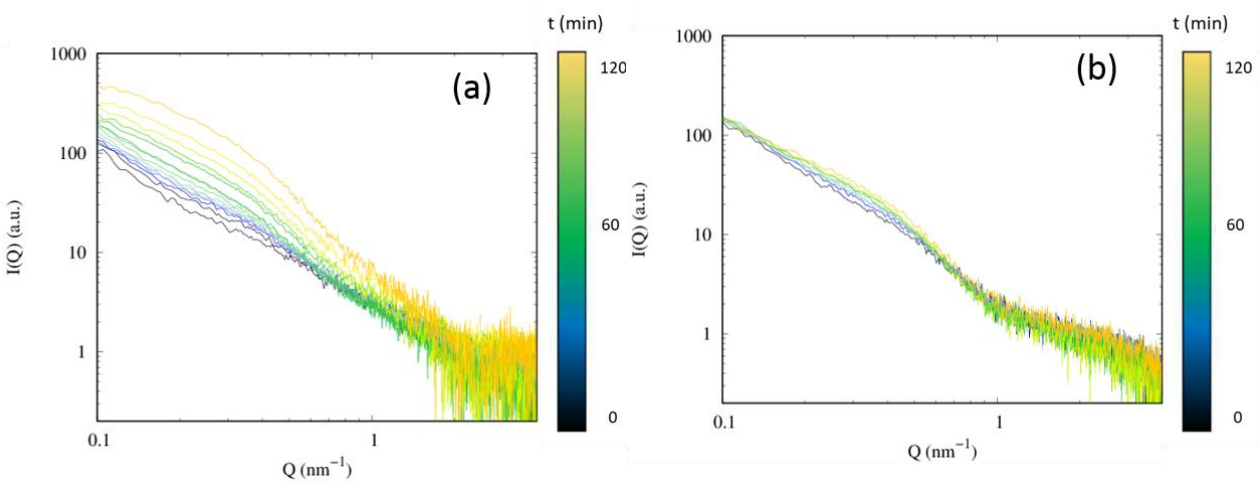

Figure 7: SAXS spectra corresponding to 200μM $A\beta_{1-42}$ aggregation at 37°C in the absence (a) and in the presence of 8μM Hsp60 (b). Colour legend corresponds to time evolution of SAXS signals

In the Kratky plot representations ($I(Q) \cdot Q^2 vs Q$) [69](Figure 8) it can be noticed that the initial states of $A\beta_{142}$ alone and together with Hsp60 suggest a different size distribution of the sample. The differences between the SAXS data reported in Figure 8 could be ascribed to the effect of the Hsp60 presence in solution. Thus, this more compact form of the $A\beta_{142}$ sample with the addition of Hsp60, as suggested by a peak at 0.4 nm^{-1}, can be attributed to the influence of Hsp60 in solution that has reduced the heterogeneity by sequestering some of the $A\beta_{142}$ oligomer species. However, both the

samples -with and without Hsp60- evolve, as already described in the ThT fluorescence experiments. After about 30 minutes, it can be observed that the SAXS curves corresponding to $A\beta_{142}$ with and without Hsp60 seen in the Kratky plots (Figure 8b), almost overlap, in agreement with the ThT results. On the other hand, the final products of aggregation from both samples are mostly compact, given their well-shaped bell form. Nonetheless, the peak of the bell, linked to the average size of the final aggregates, is slightly different, with a reduction of the size of the aggregates of about 30% in presence of the chaperonin.

This result is in agreement with fluorescence measurements, for which the differences between the samples arise only after about 90 minutes and are more evident at longer times. SAXS measurements show that Hsp60 is able to modify the kinetics of aggregation at its early stage, since differences can be already detected in the measurements performed at time 0 (Figure 8a). In addition, the chaperonin effect is observable even at high $A\beta_{142}$ concentration, for which we have since the beginning the co-presence of oligomers and monomers in solution, suggesting a mechanism of preferential binding with the low molecular weight species.

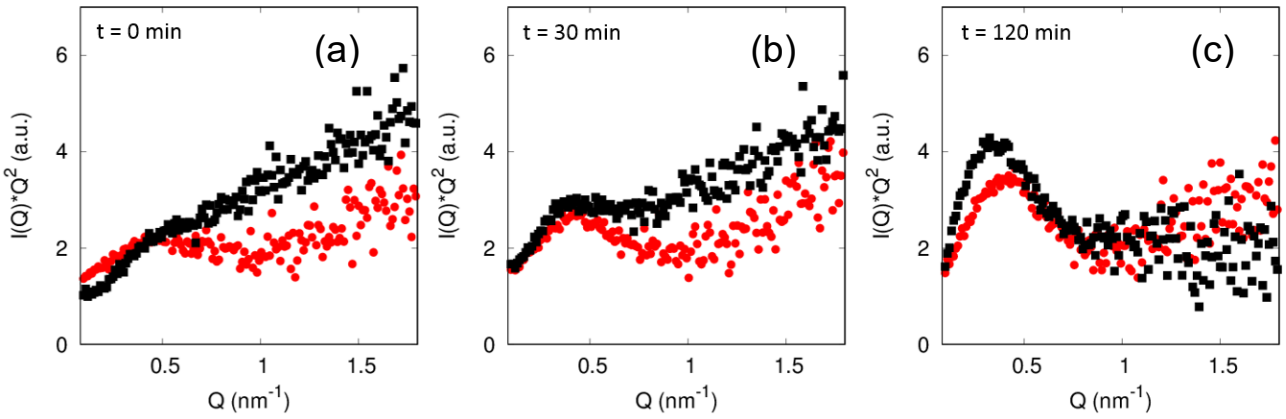

Figure 8: Kratky plots obtained from SAXS curves acquired at the starting point (a) of the kinetics of $A\beta_{1-42}$ (black) and $A\beta_{1-42}$ + Hsp60 (red), after 30 minutes (b) and at 120 minutes (c). Kratky plot relative to the final point of the kinetics is obtained by normalization at the scattering intensity at the lowest Q value.

Overall, SAXS analysis reveals that, under the high concentration condition, $A\beta_{142}$ appears to be a heterogeneous sample at the beginning of the time course. This heterogeneity triggers a more chaotic fibrillation process. It is noteworthy that the chaperonin is able to reduce the occurrence of this chaotic process, as evidenced by the reduced evolution in the scattered intensity (Figure 7). In addition, the Kratky plot indicates that the presence of Hsp60 changes the size distribution at the beginning of the kinetics (Figure 8). This is the consequence of the seeds being sequestered by Hsp60 limiting the

propagation of aggregation, reducing the heterogeneity and leading to a decrease in the aggregates size of about 30%.

3. Conclusions

Mitochondrial Hsp60 was shown to inhibiting $A\beta_{1-40}$ amyloid aggregation process and influence its toxic effect on membranes[70, 71]. In this study, we evaluate the effects of Hsp60 chaperonin on the amyloid fibrillogenesis process of the $A\beta_{1-42}$ that is more prone to aggregate and frequent in amyloid Alzheimer's Disease plaques than AD. Moreover, these effects were compared with the action exerted by GroEL, the Hsp60 bacterial homolog, that was recently shown to reduce the neurotoxic effects of $A\beta_{1-42}$ by binding its apical domain through hydrophobic interactions[37].

Our results show that Hsp60 is able to strongly inhibit also the $A\beta_{1-42}$ amyloid aggregation process and suggest that, as previously shown for $A\beta_{1-40}$, it occurs by a holding mechanism directed on $A\beta_{1-42}$ seeds, thus delaying the amyloid cascade. Thanks to the kinetics dose-dependence analysis developed for studying $A\beta_{1-42}$ aggregation inhibition[33, 35], we also show that the holding action is exerted at each of the nucleation phases, thus confirming the strong effectiveness of Hsp60 in affecting $A\beta_{1-42}$ peptide aggregation. This result is interesting due to the high toxicity of these small oligomers, which are believed to be the primary causative toxic species, and the role of these in triggering pathological aggregation. Although not jet evaluated in a cellular context, our study provides evidence of significant inhibition of $A\beta_{1-42}$ fibrillation by chaperonin interference with the pathological pathway of protein aggregation. This becomes even more true considering that, when compared with the action of GroEL, proven to protect neuronal cells from $A\beta_{1-42}$ toxic insult[37], Hsp60 is much more effective in reducing the lag phase and the growth rate than its bacterial homolog. The different amount of hydrophobic surfaces available for the ANS interaction suggests that this could be at the basis of the much greater efficiency shown by Hsp60. With the available data, it is hard to determine whether the concentration of protein segments probed by ANS is to ascribe to the existence of different exposed hydrophobic binding regions (the two proteins share only 55% of sequence[43]) or to the different oligomeric organization, being GroEL assembled as a double ring structure and mitochondrial Hsp60 mainly existing in heptamer/tetradecamer equilibrium[62]. However, although we do not directly compare chaperonins in the same quaternary structures, our study directly correlates the inhibition power to the exposure of hydrophobic regions as determined by the oligomeric equilibrium in physiological conditions. In fact, Hsp60 homo-oligomers of seven subunits of ~440,000 MW were found not only in vitro[62, 70], but also in humans[72] and in other mammals (e.g.

Hsp60 from Chinese hamster ovary (CHO)), that share a high sequence similarity with the human counterpart[73].

Also, these result further underline that the evolution from bacterial GroEL to the human homologue, Hsp60, has led to an increased efficiency of this protective action by linking the structural and dynamical differences, as already demonstrated[38, 39], with a gain in functionality. In this respect, future investigations on the effect of Hsp60 precursor, transiently present in cells, except for some pathological cancer conditions, and bearing the leader peptide as the consequence of evolutionary thrust[43], will offer new ideas and thoughts on this topic".

Overall, our results significantly increase the understanding of the interactions involved in the ability of Hsp60, and chaperones in general, to counteract pathological aggregation and, therefore, provide a foundation for potential new therapeutic strategies against the neurodegenerative pathologies sharing a commune mechanism of pathological protein aggregation[15, 28, 33, 37, 54, 57, 74].

4. Materials and Methods

Sample preparation

The synthetic peptide $A\beta_{142}$ (Anaspec) was solubilized in 5 mM NaOH (Sigma-Aldrich), pH 10, and lyophilized according to Fezoui et al.[75]. The lyophilized peptide was then dissolved in 20 mM Tris pH 7.7, 3% glycerol, 30 mM NaCl. Samples at high concentration (200 μM) were filtered using a 200 nm pore size syringe filter (Millex – LG). For samples at low concentration (≤ 50 μM) a supplementary step was realized by 50 KDa cut-off centrifuge filtration (Amicon Ultra 4 Millipore). This protocol was chosen after appropriate controls, as reported in the Supplementary Material (SM). All samples were prepared in asepsis tipically using a cold room at 4 °C. Aβ concentration was obtained by tyrosine absorption at 276 nm using an extinction coefficient of 1390 $cm^{-1}\,M^{-1}$.

The 60 kDa mitochondrial heat shock protein (Hsp60), lacking the mitochondrial import signal (MIS) of the precursor or naïve form, was purchased from ATGen in 20 mM Tris-HCl buffer (pH 8.0) and 10% glycerol containing 0.1 M NaCl and stord at − 80 °C before use. Prior to each experiment, the protein was thawed at 4 °C in a cold room. In order to obtain the protein in 20 mM Tris-HCl buffer (pH 7.7) 3% glycerol and 30 mM NaCl appropriate dilution and concentration cycles using centrifugal filter device with a cut-off of 30 kDa (Millipore Amicon – Ultra 4) were used.

Lyophilized GroEL, obtained from SIGMA (St. Louis, MO, USA), was solubilized in 20 mM Tris-HCl buffer (pH 7.7), 3% glycerol and 30 mM NaCl.

The functionality of both chaperonin stocks was evaluated by ATP activity measurements as reported elsewhere[38].

Human and bacterial chaperonins were filtered with 200 nm syringe filter (Millex LG) before use.

The stability of the protein and the absence of exogenous growth were monitored over time by Static Light Scattering measurements (data not shown). The concentration was determined by HPLC measurements.

ThT spectrofluorometric measurements

ThT fluorescence emission was monitored using a 96-well Thermo Scientific Fluoroskan Ascent F2 Microplate with thermostatic control at 37 °C. A final concentration of 12 μM ThT was used for all samples, and excitation and emission wavelengths of 450 and 485 nm, respectively. All measurements were performed in triplicate.

ANS spectrofluorometric measurements

Titration measurements for 1-anilino-8-naphthalene sulfonate (ANS) fluorescence were performed on a JASCO FP-6500 spectrofluorimeter at 20 °C. The ANS emission spectrum was measured with λ_{ex}= 380 nm using a scan rate of 100 nm min^{-1}; the excitation and emission slit width was 3 nm. Titration experiments were performed by measuring fluorescence properties of the ANS incubated in the range from 0 to 95 μM with 1 μM GroEL or Hsp60.

Atomic force microscope (AFM)

AFM measurements were performed by using a Nanowizard III (JPK Instruments, Germany) mounted on an Eclips Ti (Nikon, Japan) inverted optical microscope. Aliquots of protein solutions were deposited onto freshly cleaved mica surfaces (Agar Scientific, Assing, Italy) and incubated for up to 20 min before rinsing with deionized water and drying under a low-pressure nitrogen flow. Imaging of the protein was carried out in intermittent contact mode in air by using a NCHR silicon cantilever (Nanoworld, Switzerland) with a nominal spring constant ranging from 21 to 78 N/m, and typical resonance frequency ranging from 250 to 390 kHz.

Small Angle X Scattering (SAXS)

SAXS data of Hsp60 with $A\beta_{1-42}$ were collected at the Austrian beamline of Elettra Synchrotron in Trieste, Italy[76]. Measurements were carried out at 37°C in capillaries with 0.01 mm wall thickness made from borosilicate (Hilgenberg, Maisfeld, Germany), enclosed within a thermostatic compartment connected to an external circulation bath and a thermal probe for temperature control. We measured each sample 20 times with an acquisition time of 20 s and a rest time of 40 s for each step after a negative control for radiation damage. Two-dimensional patterns were recorded by an image plate detector. The protein macroscopic differential scattering cross section, $d\Sigma/d\Omega(Q)$, where Q is the scattering vector defined as $Q = 4\pi\, sin(2\theta)/\lambda$, 2θ is the scattering angle and $\lambda = 0.154nm$ is the wavelength, was determined by subtracting the buffer signal, corrected for its fractional volume in the solution, from the protein signal. We carefully checked each set of scattering patterns and performed the average after a positive control over radiation damage.

Acknowledgements

We are grateful to Dr. Raffaele Sinibaldi for his fundamental support for SAXS experiments. We thank Prof. Heinz Amenitsch for his technical assistance on Austrian SAXS beamline in Elettra.

We also express our sincere thanks to Jill Salvo, associate professor of biology in Union College-Schenectady, for critical and enlightening suggestions. Our thanks go to Dr. Alessia Provenzano and to Mrs. Mario Lapis and Fabrizio Giambertone for their dedicated and precious technical assistance.

Competing financial interests: The authors declare no competing financial interests

Funding: This work was supported by Italian grant FIRB “Future in research” RBFR12SIPT MIND: "Multidisciplinary Investigations for the development of Neuro-protective Drugs".

- References

1. Haass, C., and Selkoe, D. (2007) Soluble protein oligomers in neurodegeneration: Lessons from the Alzheimer's amyloid beta-peptide *Nat Rev Mol Cell Biol 8*, 101-112.
2. Glabe, C. G. (2006) Common mechanisms of amyloid oligomer pathogenesis in degenerative disease, *Neurobiol Aging 27*, 570-575.
3. Mangione, M. R., Palumbo Piccionello, A., Marino, C., Ortore, M. G., Picone, P., Vilasi, S., Di Carlo, M., Buscemi, S., D., B., and San Biagio, P. L. (2015) Photo-inhibition of Aβ fibrillation mediated by a newly designed fluorinated oxadiazole, *Rsc Adv 5*, 16540-16548.
4. Chong, Y. H., Shin, Y. J., Lee, E. O., Kayed, R., Glabe, C. G., and Tenner, A. J. (2006) ERK1/2 activation mediates Abeta oligomer-induced neurotoxicity via caspase-3 activation and tau cleavage in rat organotypic hippocampal slice cultures, *J Biol Chem 281*, 20315-20325.
5. Cizas, P., Budvytyte, R., Morkuniene, R., Moldovan, R., Broccio, M., Losche, M., Niaura, G., Valincius, G., and Borutaite, V. (2010) Size-dependent neurotoxicity of beta-amyloid oligomers, *Archives of biochemistry and biophysics 496*, 84-92.
6. Kayed, R., and Lasagna-Reeves, C. A. (2013) Molecular mechanisms of amyloid oligomers toxicity, *Journal of Alzheimer's disease : JAD 33 Suppl 1*, S67-78.
7. Gaspar, R. C., Villarreal, S. A., Bowles, N., Hepler, R. W., Joyce, J. G., and Shughrue, P. J. (2010) Oligomers of beta-amyloid are sequestered into and seed new plaques in the brains of an AD mouse model, *Experimental Neurology 223*, 394-400.
8. Takahashi, R. H., Almeida, C. G., Kearney, P. F., Yu, F., Lin, M. T., Milner, T. A., and Gouras, G. K. (2004) Oligomerization of Alzheimer's beta-amyloid within processes and synapses of cultured neurons and brain, *J Neurosci 24*, 3592-3599.
9. Ellis, R. J. (2003) Protein folding: importance of the Anfinsen cage, *Current Biology 13*, R881- R883.
10. Ellis, R. J. (2006) Molecular chaperones: assisting assembly in addition to folding, *trends biochem sci*, 395 - 401.
11. Ellis, R. J. (2003) Molecular chaperones: Plugging the transport gap, *Nature 421*, 801-802.
12. Frydman, J. (2001) FOLDING OF NEWLY TRANSLATED PROTEINS IN VIVO: The Role ofMolecular Chaperones, *Annual review of biochemistry 70*, 603-647.
13. Schlieker, C., Bukau, B., and Mogk, A. (2002) Prevention and reversion of protein aggregation by molecular chaperones in the E-coli cytosol: implications for their applicability in biotechnology, *Journal of Biotechnology 96*, 13-21.
14. Muchowski, P. J., and Wacker, J. L. (2005) Modulation of neurodegeneration by molecular chaperones, *Nat Rev Neurosci 6*, 11-22.
15. Aprile, F. A., Kallstig, E., Limorenko, G., Vendruscolo, M., Ron, D., and Hansen, C. (2017) The molecular chaperones DNAJB6 and Hsp70 cooperate to suppress alpha-synuclein aggregation, *Scientific reports 7*, 9039.
16. Mogk, A., Bukau, B., Kampinga, H.H. (2018) cellular handling of protein aggreegates by disaggregation machines, *Molecular Cell 69*, 214-226.
17. Chiti, F., and Dobson, C. M. (2006) Protein misfolding, functional amyloid, and human disease, *Annual review of biochemistry 75*, 333-366.
18. Bourdenx, M., Koulakiotis, N. S., Sanoudou, D., Bezard, E., Dehay, B., and Tsarbopoulos, A. (2017) Protein aggregation and neurodegeneration in prototypical neurodegenerative diseases: Examples of amyloidopathies, tauopathies and synucleinopathies, *Prog Neurobiol 155*, 171-193.
19. Carrotta, R., Canale, C., Diaspro, A., Trapani, A., Biagio, P. L. S., and Bulone, D. (2012) Inhibiting effect of α s1-casein on Aβ 1-40 fibrillogenesis., *Biochimica et Biophysica Acta - General Subjects 1820*, 124-132.
20. Ben-Zvi, A. P., and Goloubinoff, P. (2001) Review: Mechanisms of disaggregation and refolding of stable protein aggregates by molecular chaperones, *Journal of structural biology 135*, 84-93.
21. Braig, K. (1998) Chaperonins, *Current opinion in structural biology 8*, 159-165.

22. Piana, S., and Shaw, D. E. (2018) Atomic-Level Description of Protein Folding inside the GroEL Cavity, *The journal of physical chemistry. B*.
23. Sot, B., Rubio-Munoz, A., Leal-Quintero, A., Martinez-Sabando, J., Marcilla, M., Roodveldt, C., and Valpuesta, J. M. (2017) The chaperonin CCT inhibits assembly of alpha-synuclein amyloid fibrils by a specific, conformation-dependent interaction, *Scientific reports 7*, 40859.
24. Mangione, M. R., Vilasi, S., Marino, C., Librizzi, F., Canale, C., Spigolon, D., Bucchieri, F., Fucarino, A., Passantino, R., Cappello, F., Bulone, D., and San Biagio, P. L. (2016) Hsp60, amateur chaperone in amyloid-beta fibrillogenesis, *Biochim Biophys Acta 1860*, 2474-2483.
25. Ricci, C., Maccarini, M., Falus, P., Librizzi, F., Mangione, M. R., Moran, O., Ortore, M. G., Schweins, R., Vilasi, S., and Carrotta, R. (2019) Amyloid beta-Peptides Interaction with Membranes: Can Chaperones Change the Fate?, *The journal of physical chemistry. B 123*, 631-638.
26. Barral, J. M., Broadley, S. A., Schaffar, G., and Hartl, F. U. (2004) Roles of molecular chaperones in protein misfolding diseases, *Seminars in cell & developmental biology 15*, 17-29.
27. Cohen, F. E., and Kelly, J. W. (2003) Therapeutic approaches to protein-misfolding diseases, *Nature 426*, 905-909.
28. Paul, S., and Mahanta, S. (2014) Association of heat-shock proteins in various neurodegenerative disorders: is it a master key to open the therapeutic door?, *Mol Cell Biochem 386*, 45-61.
29. Meisl, G., Yang, X., Hellstrand, E., Frohm, B., Kirkegaard, J. B., Cohen, S. I., Dobson, C. M., Linse, S., and Knowles, T. P. (2014) Differences in nucleation behavior underlie the contrasting aggregation kinetics of the Abeta40 and Abeta42 peptides, *Proc Natl Acad Sci U S A 111*, 9384-9389.
30. Dovidchenko, N. V., Glyakina, A. V., Selivanova, O. M., Grigorashvili, E. I., Suvorina, M. Y., Dzhus, U. F., Mikhailina, A. O., Shiliaev, N. G., Marchenkov, V. V., Surin, A. K., and Galzitskaya, O. V. (2016) One of the possible mechanisms of amyloid fibrils formation based on the sizes of primary and secondary folding nuclei of Abeta40 and Abeta42, *Journal of structural biology 194*, 404-414.
31. Sengupta, U., Nilson, A. N., and Kayed, R. (2016) the role of amyloid-b oligomers in toxicity, propagation, and immunoterapy, *EBioMedicine 6*, 42-49.
32. Selivanova, O. M., Surin, A. K., Marchenkov, V. V., Dzhus, U. F., Grigorashvili, E. I., Suvorina, M. Y., Glyakina, A. V., Dovidchenko, N. V., and Galzitskaya, O. V. (2016) The Mechanism Underlying Amyloid Polymorphism is Opened for Alzheimer's Disease Amyloid-beta Peptide, *J Alzheimers Dis 54*, 821-830.
33. Månsson, C., Arosio, P., Hussein, R., Kampinga, H. H., Hashem, R. M., Boelens, W. C., Dobson, C. M., Knowles, T. P., Linse, S., and C., E. (2014) Interaction of the molecular chaperone DNAJB6 with growing amyloid-beta 42 (Aβ42) aggregates leads to sub-stoichiometric inhibition of amyloid formation, *J Biol Chem. 289*, 31066-31076.
34. Meisl, G., Kirkegaard, J. B., Arosio, P., Michaels, T. C., Vendruscolo, M., Dobson, C. M., Linse , S., and Knowles, T. P. (2016) Molecular mechanisms of protein aggregation from global fitting of kinetic models, *Nat Protoc. 11*.
35. Arosio, P., Michaels, T. C., Linse, S., Mansson, C., Emanuelsson, C., Presto, J., Johansson, J., Vendruscolo, M., Dobson, C. M., and Knowles, T. P. (2016) Kinetic analysis reveals the diversity of microscopic mechanisms through which molecular chaperones suppress amyloid formation, *Nat Commun 7*, 10948.
36. Yagi-Utsumi, M., Kunihara, T., Nakamura, T., Uekusa, Y., Makabe, K., Kuwajima, K., and Kato, K. (2013) NMR characterization of the interaction of GroEL with amyloid β as a model ligand., *FEBS Letters 587*, 1605-1609.
37. Walti, M. A., Steiner, J., Meng, F., Chung, H. S., Louis, J. M., Ghirlando, R., Tugarinov, V., Nath, A., and Clore, G. M. (2018) Probing the mechanism of inhibition of amyloid-beta(1-42)-induced neurotoxicity by the chaperonin GroEL, *Proc Natl Acad Sci U S A 115*, E11924-E11932.
38. Ricci, C., Ortore, M. G., Vilasi, S., Carrotta, R., Mangione, M. R., Bulone, D., Librizzi, F., Spinozzi, F., Burgio, G., Amenitsch, H., and San Biagio, P. L. (2016) Stability and disassembly properties of human naive Hsp60 and bacterial GroEL chaperonins, *Biophys Chem 208*, 68-75.
39. Ricci, C., Carrotta, R., Rappa, G. C., Mangione, M. R., Librizzi, F., San Biagio, P. L., Amenitsch, H., Ortore, M. G., and Vilasi, S. (2017) Investigation on different chemical stability of mitochondrial Hsp60 and its precursor, *Biophys Chem 229*, 31-38.

40. Spinello, A., Ortore, M. G., Spinozzi, F., Ricci, C., Barone, G., Gammazza, A. M., and Piccionello, A. P. (2015) Quaternary structures of GroEL and naive-Hsp60 chaperonins in solution: a combined SAXS-MD study, *Rsc Adv 5*, 49871-49879.
41. Vilasi, S., Carrotta, R., Mangione, M. R., Campanella, C., Librizzi, F., Randazzo, L., Martorana, V., Gammazza, A. M., Ortore, M. G., Vilasi, A., Pocsfalvi, G., Burgio, G., Corona, D., Piccionello, A. P., Zummo, G., Bulone, D., de Macario, E. C., Macario, A. J. L., San Biagio, P. L., and Cappello, F. (2014) Human Hsp60 with Its Mitochondrial Import Signal Occurs in Solution as Heptamers and Tetradecamers Remarkably Stable over a Wide Range of Concentrations, *Plos One 9*.
42. Slavotinek, A. M., and Biesecker, L. G. (2001) Unfolding the role of chaperones and chaperonins in human disease, *Trends in genetics : TIG 17*, 528-535.
43. Tikhomirova, T. S., and Galzitskaya, O. V. (2018) [Functionally Significant Amino Acid Motifs of Heat Shock Proteins: Structural and Bioinformatics Analyses of Hsp60/Hsp10 in Five Classes of Chordata], *Mol Biol (Mosk) 52*, 879-897.
44. Manczak, M., Anekonda, T. S., Henson, E., Park, B. S., Quinn, J., and Reddy, P. H. (2006) Mitochondria are a direct site of A beta accumulation in Alzheimer's disease neurons: implications for free radical generation and oxidative damage in disease progression, *Hum Mol Genet 15*, 1437-1449.
45. Du, H., Guo, L., Yan, S., Sosunov, A. A., McKhann, G. M., and Yan, S. S. (2010) Early deficits in synaptic mitochondria in an Alzheimer's disease mouse model, *Proceedings of the National Academy of Sciences of the United States of America 107*, 18670-18675.
46. Chandra, D., Choy, G., and Tang, D. G. (2007) Cytosolic accumulation of HSP60 during apoptosis with or without apparent mitochondrial release: Evidence that its pro-apoptotic or pro-survival functions involve differential interactions with caspase-3., *Journal of Biological Chemistry 282*, 31289-31301.
47. Soltys, B. J., and Gupta, R. S. (1998) Mitochondrial molecular chaperones hsp60 and mhsp70: are their role restricted to mitochondria?. In *Stress Proteins* (Latchman, D. S., Ed.), pp 69 - 100, Springer.
48. Merendino, A. M., Bucchieri, F., Campanella, C., Marcianò, V., Ribbene, A., David, S., Zummo, G., Burgio, G., Corona, D. F. V., Conway de Macario, E., Macario, A. J. L., and Cappello, F. (2010) Hsp60 is actively secreted by human tumor cells., *Plos One 5*, e9247.
49. Campanella, C., Bucchieri, F., Merendino, A. M., Fucarino, A., Burgio, G., Corona, D. F. V., Barbieri, G., David, S., Farina, F., Zummo, G., Conway de Macario, E., Macario, A. J. L., and Cappello, F. (2012) The odyssey of Hsp60 from tumor cells to other destinations includes plasma membrane-associated stages and Golgi and exosomal protein-trafficking modalities., *Plos One 7*, e42008.
50. Nichols, M. R., Moss, M. A., Reed, D. K., Cratic-McDaniel, S., Hoh, J. H., and Rosenberry, T. L. (2005) Amyloid-beta protofibrils differ from amyloid-beta aggregates induced in dilute hexafluoroisopropanol in stability and morphology, *J Biol Chem 280*, 2471-2480.
51. Corsale, C., Carrotta, R., Mangione, M. R., Vilasi, S., Provenzano, A., Cavallaro, G., Bulone, D., and San Biagio, P. L. (2012) Entrapment of Aβ 1-40 peptide in unstructured aggregates., *Journal of Physics Condensed Matter 24*, 244103.
52. Suvorina, M. Y., Selivanova, O. M., Grigorashvili, E. I., Nikulin, A. D., Marchenkov, V. V., Surin, A. K., and Galzitskaya, O. V. (2015) Studies of Polymorphism of Amyloid-beta42 Peptide from Different Suppliers, *Journal of Alzheimer's disease : JAD 47*, 583-593.
53. Bitan, G., and Teplow, D. B. (2005) *Preparation of Aggregate-Free, Low Molecular Weight Amyloid-β for Assembly and Toxicity Assays*, Sigurdsson E.M. .
54. Narayan, P., Orte, A., Clarke, R. W., Bolognesi, B., Hook, S., Ganzinger, K. A., Meehan, S., Wilson, M. R., Dobson, C. M., and Klenerman, D. (2011) The extracellular chaperone clusterin sequesters oligomeric forms of the amyloid-beta(1-40) peptide, *Nat Struct Mol Biol 19*, 79-83.
55. Wilhelmus, M. M. M., de Waal, R. M. W., and Verbeek, M. M. (2007) Heat Shock Proteins and Amateur Chaperones in Amyloid-Beta Accumulation and Clearance in Alzheimer's Disease, *Molecular Neurobiology 35*, 203-216.
56. Librizzi, F., Carrotta, R., Spigolon, D., Bulone, D., and San Biagio, P. L. (2014) alpha-Casein Inhibits Insulin Amyloid Formation by Preventing the Onset of Secondary Nucleation Processes, *The journal of physical chemistry letters 5*, 3043-3048.

57. Behrends, C., Langer, C. A., Boteva, R., Bottcher, U. M., Stemp, M. J., Schaffar, G., Rao, B. V., Giese, A., Kretzschmar, H., Siegers, K., and Hartl, F. U. (2006) Chaperonin TRiC promotes the assembly of polyQ expansion proteins into nontoxic oligomers, *Mol Cell 23*, 887-897.
58. Ojha, B., Fukui, N., Hongo, K., Mizobata, T., and Kawata, Y. (2016) Suppression of amyloid fibrils using the GroEL apical domain, *Scientific reports 6*.
59. Cardamone, M., and Puri, N. K. (1992) Spectrofluorimetric assessment of the surface hydrophobicity of proteins, *The Biochemical journal 282 (Pt 2)*, 589-593.
60. Carrotta, R., Manno, M., Giordano, F. M., Longo, A., Portale, G., Martorana, V., and Biagio, P. L. (2009) Protein stability modulated by a conformational effector: effects of trifluoroethanol on bovine serum albumin, *Physical chemistry chemical physics : PCCP 11*, 4007-4018.
61. Nielsen, K. L., and Cowan, N. J. (1998) A single ring is sufficient for productive chaperonin-mediated folding in vivo., *Molecular Cell 2*, 93-99.
62. Parnas, A., Nadler, M., Nisemblat, S., Horovitz, A., Mandel, H., and Azem, A. (2009) The MitCHAP-60 disease is due to entropic destabilization of the human mitochondrial Hsp60 oligomer., *Journal of Biological Chemistry 284*, 28198-28203.
63. Viitanen, P. V., Lorimer, G. H., Seetharam, R., Gupta, R. S., Oppenheim, J., Thomas, J. O., and Cowan, N. J. (1992) Mammalian mitochondrial chaperonin 60 functions as a single toroidal ring., *Journal of Biological Chemistry 267*, 695-698.
64. Cappello, F., Caramori, G., Campanella, C., Vicari, C., Gnemmi, I., Zanini, A., Spanevello, A., Capelli, A., la Rocca, G., Anzalone, R., Bucchieri, F., D'Anna, S. E., Ricciardolo, F. L. M., Brun, P., Balbi, B., Carone, M., Zummo, G., Conway de Macario, E., Macario, A. J. L., and Di Stefano, A. (2011) Convergent sets of data from In Vivo and In Vitro methods point to an active role of Hsp60 in chronic obstructive pulmonary disease pathogenesis., *Plos One 6*, e28200.
65. Joachimiak, L. A., Walzthoeni, T., Liu, C. W., Aebersold, R., and Frydman, J. (2014) The structural basis of substrate recognition by the eukaryotic chaperonin TRiC/CCT, *Cell 159*, 1042-1055.
66. Lin, P. Y., Simon, S. M., Koh, W. K., Folorunso, O., Umbaugh, C. S., and Pierce, A. (2013) Heat shock factor 1 over-expression protects against exposure of hydrophobic residues on mutant SOD1 and early mortality in a mouse model of amyotrophic lateral sclerosis, *Molecular neurodegeneration 8*, 43.
67. Ellis, R. J., and van der Vies, S. M. (1991) Molecular Chaperones, *ann rev biochem 60*, 321-347.
68. Glatter, O., and O., k. (1982) Small angle x-ray scattering, *London: Academic Press Inc. Ltd.*
69. Pilz, I., Glatter, O., and Kratky, O. (1979) Small-angle X-ray scattering. , *Methods Enzymol. 61*, 148-249.
70. Mangione, M. R., Vilasi, S., Marino, C., Librizzi, F., Canale, C., Spigolon, D., Bucchieri, F., Fucarino, A., Passantino, R., Cappello, F., Bulone, D., and San Biagio, P. L. (2016) Hsp60, amateur chaperone in amyloid-beta fibrillogenesis, *Bba-Gen Subjects 1860*, 2474-2483.
71. Ricci, C., Maccarini, M., Falus, P., Librizzi, F., Mangione, M. R., Moran, O., Ortore, M. G., Schweins, R., Vilasi, S., and Carrotta, R. (2018) Amyloid beta-Peptides Interaction with Membranes: Can Chaperones Change the Fate?, *The journal of physical chemistry. B*.
72. Jindal, S., Dudani, A. K., Singh, B., Harley, C. B., and Gupta, R. S. (1989) Primary structure of a human mitochondrial protein homologous to the bacterial and plant chaperonins and to the 65-kilodalton mycobacterial antigen., *Molecular and Cellular Biology 9*, 2279-2283.
73. Picketts, D. J., Mayanil, C. S., and Gupta, R. S. (1989) Molecular cloning of a Chinese hamster mitochondrial protein related to the "chaperonin" family of bacterial and plant proteins, *The Journal of biological chemistry 264*, 12001-12008.
74. Bross, P., Magnoni, R., and Bie, A. S. (2012) Molecular chaperone disorders: defective Hsp60 in neurodegeneration, *Current topics in medicinal chemistry 12*, 2491-2503.
75. Fezoui, Y., Hartley, D. M., Harper, J. D., Khurana, R., Walsh, D. M., Condron, M. M., Selkoe, D. J., Lansbury Jr., P. T., Fink, A. L., and Teplow, D. B. (2000) An improving method of preparing the amyloid β-protein for fibrillogenesis and neurotoxicity experiments, *Amyloid: Int. J. Exp. Clin. Invest. 7*, 166-178.

76. Amenitsch, H., Rappolt, M., Kriechbaum, M., Mio, H., Laggner, P., and Bernstorff, S. (1998) First performance assessment of the small-angle X-ray scattering beamline at ELETTRA, *Journal of synchrotron radiation 5*, 506-508.